

Quasi-Ballistic Transport in Nanowire Field-Effect Transistors

Giorgio Baccarani, Elena Gnani, Antonio Gnudi, Susanna Reggiani

Abstract—In this work we investigate quasi-ballistic transport in nanowire field-effect transistors (NW-FETs) by addressing the 1D Boltzmann transport equation. First, we find its *exact* analytical solution for any potential profile within the constraint of dominant elastic scattering. Next, we calculate the *I-V* characteristics of the NW-FET, which differ from the Landauer expression for the inclusion of a transmission coefficient smaller than one. Our approach provides a methodology for the calculation of the transmission and backscattering coefficients directly from the scattering probabilities. These coefficients turn out to be functions of the ratio between the device length and a suitably-averaged momentum-relaxation distance. One of the main conclusions of the paper is that, so long as inelastic collisions are neglected, the so-called *kT*-layer plays no role in 1D devices.

I. INTRODUCTION

Ballistic and quasi-ballistic transport in silicon planar MOS-FETs and nanowire (NW) FETs has been the subject of many investigations. Most papers tackle the problem numerically, often using transport models which address either the Boltzmann transport equation (BTE) by Monte Carlo and deterministic techniques, or the open-boundary Schrödinger equation. To date, there is a general consensus on the conclusion that the role of scattering is never negligible, at least quantitatively, even at the shortest channel lengths [1].

In this paper, we work out an *exact* analytical solution of the 1D BTE under the assumption of negligible optical-phonon (OP) scattering. This solution allows us to work out closed-form expressions for the current and carrier concentration in NW-FETs at the computational cost of a numerical integral for every energy and bias point. The potential profile along the channel is computed by numerically solving the coupled Schrödinger-Poisson equations. Self-consistency is achieved by iteration of the procedure.

This paper is organized as follows: in Section II we develop the analytical solution of the 1D BTE under general potential profiles along the nanowire. In Section III the *I-V* characteristics are worked out and compared with results provided by a numerical BTE solver. Also, a procedure for the calculation of the transmission and backscattering coefficients is outlined. Conclusions are drawn in Section IV.

II. BTE SOLUTION WITH QUASI-BALLISTIC TRANSPORT

In this section we address the solution of the 1D BTE within a NW-FET under quasi-ballistic transport conditions. In doing so, however, we do not rely on McKelvey's flux

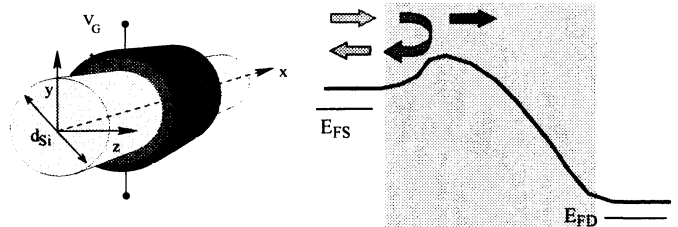


Fig. 1. Left: Schematic representation of a gate-all-around cylindrical nanowire FET. Right: Typical subband-edge profile along a nanowire FET.

theory [2] as was done in previous works [3]–[7] but, rather, determine the appropriate boundary conditions to be applied to the distribution function for both positive and negative velocities. So doing, we need not splitting the BTE in two coupled equations for f^+ and f^- , and succeed in finding its *exact* solution within the constraint of purely-elastic collisions. Figure 1 shows a sketch of a cylindrical NW-FET and the typical space dependence of the first subband edge, referred to as $E_c(x)$. In our approach, scattering events are accounted for via the relaxation-time approximation (RTA), which holds for elastic collisions only. It may be shown that the RTA is actually exact in 1D for intra-subband scattering, and that inter-subband scattering can be approximately emulated by intra-subband scattering by applying suitable weighting factors to the scattering rates. Assuming negligible inelastic collisions, the RTA is valid even beyond the onset of degeneracy, since the terms accounting for the exclusion principle within the scattering integral cancel out. The BTE thus takes the usual form

$$u_x \frac{\partial f}{\partial x} - \frac{q}{\hbar} \mathcal{E}_x \frac{\partial f}{\partial k_x} = -\frac{f - f_0}{\tau(x, k_x)} \quad (1)$$

but $f_0(x, k_x)$ represents in this case the even part of $f(x, k_x)$. Under the assumption of purely-elastic scattering, $f_0(x, k_x)$ is no longer the local equilibrium distribution function, for energy relaxation is ruled out. Therefore, isoenergetic collisions cannot change the energy distribution, but can only affect the momentum distribution of the carriers. Indicating with $f_0(x, k_x)$ and $f_1(x, k_x)$ the even and odd parts of $f(x, k_x)$, respectively, and recognizing that the even and odd terms of (1) must separately balance, we find the system of equations

$$u_x \frac{\partial f_0}{\partial x} - \frac{q}{\hbar} \mathcal{E}_x \frac{\partial f_0}{\partial k_x} = -\frac{f_1}{\tau(x, k_x)} \quad (2)$$

$$u_x \frac{\partial f_1}{\partial x} - \frac{q}{\hbar} \mathcal{E}_x \frac{\partial f_1}{\partial k_x} = 0 \quad (3)$$

where (3) is independent of $f_0(x, k_x)$ and takes the standard form of the 1D BTE with a vanishing collision integral. As

“E. De Castro” Advanced Research Center on Electronic Systems (ARCES), and Dept. of Electronics, University of Bologna, Italy.

is known, any function of the hamiltonian $F_1(H)$, with $H = E_c(x) + \varepsilon(k_x)$ fulfills equation (3). However, $H(x, k_x)$ is an even function of k_x while $f_1(x, k_x)$ is an odd function of k_x . Therefore, with reference to the inflow from the source contact, the solution of (3) is

$$f_1(x, k_x) = \frac{k_x}{|k_x|} F_1(H) \quad (4)$$

which is clearly odd. The factor $(k_x/|k_x|) = \pm 1$ according to whether $k_x > 0$ or $k_x < 0$, respectively. The odd part of the distribution function $f_1(x, k_x)$ retains the functional dependence on H imposed by the boundary condition at the source contact. However, being $H(x, k_x) = E_c(x) + \varepsilon(k_x)$, the functional dependence of $f_1(x, k_x)$ upon position and momentum is expressed via $H(x, k_x)$. The invariance of f_1 at constant H is a somewhat surprising result due to the combined effect of our assumption of purely-elastic scattering and to the general principle of current conservation. If electrons always travel at constant energy across the nanowire FET, then current conservation is required at every energy.

With $f_1(x, k_x)$ known, it is now possible to address the solution of (2). To this purpose, we set $f_0(x, k_x) = F_0(x, H)$. This definition is legitimate since f_0 is an even function of k_x . We thus find the equation

$$u_x \frac{\partial F_0}{\partial x} = -\frac{1}{\tau} \frac{k_x}{|k_x|} F_1(H) \quad (5)$$

the solution of which is

$$F_0(x, H) = F_0(0, H) - F_1(H) \int_0^x \frac{dx'}{|u_x| \tau(x, k_x)} \quad (6)$$

$$= F_0(0, H) - F_1(H) \frac{x}{\lambda_x} \quad (7)$$

The integral on the r.h.s. of (6) requires $E_c(x)$ to be known since both u_x and τ are functions of $\varepsilon = H - E_c(x)$. By defining the carrier mean-free path $\lambda = |u_x| \tau$, equation (7) holds if a suitable average λ_x is taken between 0 and x . Referring again to the inflow from the source contact, the boundary conditions $F_0(0, H)$ and $F_1(H)$ can be found by imposing $f(0, k_x) = F_S(H)$ for $k_x > 0$ and $f(L, k_x) = 0$ for $k_x < 0$. A third relationship comes from (6) at $x = L$. This leads to a set of three equations in the unknowns $F_0(0, H)$, $F_0(L, H)$ and $F_1(H)$, the solution of which is

$$F_0(0, H) = F_S(H) \frac{\tau_{av} + \tau_t}{2\tau_{av} + \tau_t} \quad (8)$$

$$F_0(L, H) = F_S(H) \frac{\tau_{av}}{2\tau_{av} + \tau_t} \quad (9)$$

$$F_1(H) = F_S(H) \frac{\tau_{av}}{2\tau_{av} + \tau_t} \quad (10)$$

where τ_t is the transit time for electrons with total energy H and $1/\tau_{av}$ is the inverse relaxation time averaged along the electron path from the source to drain contacts with $|u_x|^{-1}$ as a weighting function, namely

$$\frac{1}{\tau_{av}} = \left\{ \int_0^L \frac{dx}{|u_x|} \right\}^{-1} \int_0^L \frac{dx}{|u_x| \tau(x, k_x)} \quad (11)$$

L being the device length. The resulting average relaxation time is itself a function of H . By defining $1/\lambda_{av}$ as the

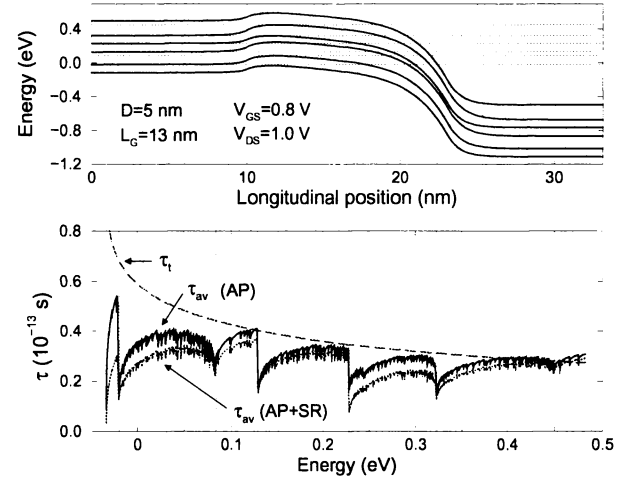


Fig. 2. Top: Position dependence of the lowest six subband edges for $V_{GS} = 0.8$ V and $V_{DS} = 1$ V across a NW-FET with diameter $d = 5$ nm and gate length $L_g = 13$ nm. Bottom: Comparison of the electron transit time τ_t and the average relaxation time τ_{av} versus total energy H . The discontinuities of τ_{av} at four energies are due to the crossing of the second, third, fourth and fifth subband edges at the source contact.

average value of $1/\lambda$ from 0 to L , $\tau_t/\tau_{av} = L/\lambda_{av}$ so that the above ratios can be used interchangeably. The distribution function for $H > E_c(x_m)$, x_m being the position of the maximum potential energy referred to as *virtual source*, is thus $f(x, k_x) = F_0(x, H) \pm F_1(H)$.

Electrons departing from the source contact with an energy smaller than the barrier height, i.e. $H < E_c(x_m)$, are reflected back to the source and do not contribute to the current. In this case, the integral on the r.h.s. of (6) extends from 0 to the turning point x_r such that $E_c(x_r) = H$, and back. Therefore, the distribution function is $f(x, k_x) = F_S(H)$ for either positive and negative values of k_x . It may thus be concluded that the distribution function of electrons with energy $H < E_c(x_m)$ is entirely set by the boundary condition. If electrons enter the nanowire with an equilibrium distribution, they will retain such a distribution in the whole region at the left of the virtual source x_m . Similar considerations can be worked out for electrons entering the NW-FET from the drain side. For the sake of brevity, we do not report this treatment, which leads to the same equations as before, with the interchange of the 0 and L sections.

The computation of the distribution function starts from the definition of the scattering probability in the nanowire induced by acoustic phonons and surface roughness. We then integrate these terms over all final states, and find the inverse relaxation times for both scattering mechanisms in the fourfold and twofold degenerate valleys of the conduction band. Next, we compute the average value of the inverse relaxation time τ_{av}^{-1} weighted by the inverse velocity $|u_x|^{-1}$ according to equation (11), and the transit time τ_t for any value of the energy $H > E_c(x_m)$ along the electron trajectory. Both τ_{av} and τ_t are plotted in figure 2 for a 5 nm diameter FET. The small negative wiggles are due to the intersections of the constant energy H with the second and higher subbands. At the intersection points the scattering probability diverges due to the 1D behavior of

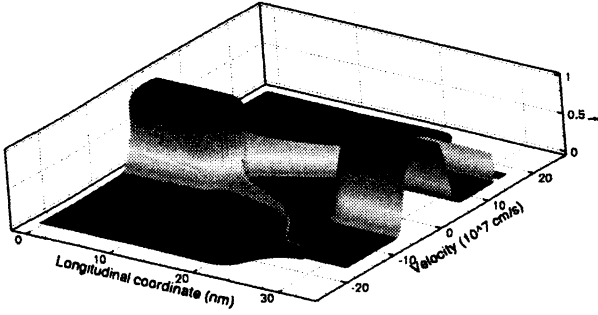


Fig. 3. Perspective plot of the distribution function versus position and velocity for the 5 nm FET. The computation is carried out at $V_{GS} = 0.8$ V and $V_{DS} = 1.0$ V.

the density of states and the size of the wiggles is related with the discrete mesh in space and energy. The mesh spacing we typically use is $\Delta x = 0.2$ nm and $\Delta E = 0.5$ meV. By reducing the mesh spacing, the size of the wiggles reduces as well, and the curve tends to its upper envelope.

The strong discontinuities in figure 2 are due to the crossing of different subbands, which are nearly flat in the source region, as shown in the upper part of the figure. Therefore, the integral of $1/\tau$ takes a very large value due to the large density of states near the subband bottom, and its inverse drops down. The transit time exhibits instead a regular behavior, and decreases monotonically as the energy H increases, as expected. It may be interesting to notice that, while τ_{av} and τ_t are roughly comparable in the high-energy region, at the lower energies $\tau_{av} < \tau_t$, indicating that some collisions are expected to occur for low-energy electrons.

Figure 3 shows a perspective plot of the distribution function $f(x, u_x)$ versus position and velocity for the 5 nm FET. The computation is carried out at $V_{GS} = 0.8$ V and $V_{DS} = 1.0$ V. This plot indicates that the majority of electrons travels with positive velocity at the source side of the channel for this device and that a only smaller portion is backscattered. The vanishing value of $f(L, u_x)$ for $u_x < 0$ imposed by the boundary condition is also clearly visible from the figure.

III. CURRENT AND CARRIER CONCENTRATION IN THE NANOWIRE

The contribution of one subband to the nanowire current requires only the knowledge of the odd part of the distribution function. If we assume that electrons enter the source contact with a Fermi distribution function, we find

$$I'_D = \frac{2qk_B T}{h} R_t \ln \left\{ 1 + \exp \left(\frac{E_{FS} - E_c(x_m)}{k_B T} \right) \right\} \quad (12)$$

which is basically Landauer's formula [8] for the nanowire current. In this expression the density of states and the group velocity cancel out any dependence of the first factor upon the effective mass, so that the latter turns out to be a universal constant. The transmission coefficient is defined as the statistical average $R_t = \langle 2\tau_{av} / (2\tau_{av} + \tau_t) \rangle$ weighted by the Fermi function. When the contribution to the current of the electrons coming from the drain is considered, equation (12) is modified

as follows

$$I'_D = \frac{2qk_B T}{h} R_t \ln \left\{ \frac{1 + \exp \{ [E_{FS} - E_c(x_m)] / k_B T \}}{1 + \exp \{ [E_{FD} - E_c(x_m)] / k_B T \}} \right\} \quad (13)$$

and $E_{FD} = E_{FS} - qV_{DS}$. So far we have been considering only the contribution from one subband to the nanowire current. By neglecting inter-subband interactions, the total drain current I_{DS} may thus be expressed as a sum of terms like (13). A nice property of (13) is that the current reverses if we exchange the source and drain contacts, as is supposed to be for a symmetric structure.

The transmission coefficient may also be expressed as $R_t = 2\lambda_p / (2\lambda_p + L)$, where λ_p can be regarded as the elastic-scattering mean-free path. This coefficient tends to 1 if the channel length $L \ll 2\lambda_p$ since, in this limit, the number of scattering events is negligible and the transport is near ballistic. In the opposite limit, instead, this factor tends to 0 since the large number of scattering events re-establishes the symmetry of the distribution function. However, before this limit is reached, the transit time would become comparable with the energy relaxation time, at which point the transport becomes dominated by drift-diffusion and the present solution would break down.

The reflection, or backscattering coefficient R_r can easily be extracted from the transmission coefficient, being its complement to 1, i.e. $R_r = 1 - R_t = L / (2\lambda_p + L)$. Although quasi-ballistic transport has been thoroughly investigated in the literature [3]–[7], this theory provides for the first time a methodology for the quantitative computation of transmission and reflection coefficients from the basic scattering probabilities. In the literature, the backscattering coefficient is usually extracted from the low-field mobility value. This methodology, however, does not consider that the scattering rate is heavily affected by the high average energy of the carriers.

Compared with previous work by Lundstrom and coworkers [3]–[7], our definition of transmission and reflection coefficients is somewhat different. Our formulation of the problem based on the calculation of Landauer's formula, suggests us to define R_t as the ratio of the net electron flows with and without backscattering. The two situations are characterized by the same positive flow injected from the source, but the charge densities would be different due to the additional negative flow generated by backscattering. In the above references, instead, the transmission coefficient is defined for a constant charge density at the virtual source and, with this definition, it is found to be (using our notation) $R'_t = (1 - R_r) / (1 + R_r)$. At constant charge, R'_t is in fact reduced both by the lower positive flow and by the negative contribution to the current of backscattered carriers. If we reconcile our definition of R_t with that in Ref. [3] by inserting the electron concentration at the virtual source into equation (13), the transmission coefficient at constant charge density would become $R'_t = \lambda_p / (\lambda_p + L)$. Figure 4 shows the turn-on characteristics, both in log and linear plots, of a 3 nm diameter FET with a gate length $L_g = 13$ nm and a drain voltage $V_{DS} = 1.0$ V. The results of the present model are compared with those of a numerical BTE solver [9], which fully accounts for the subband coupling

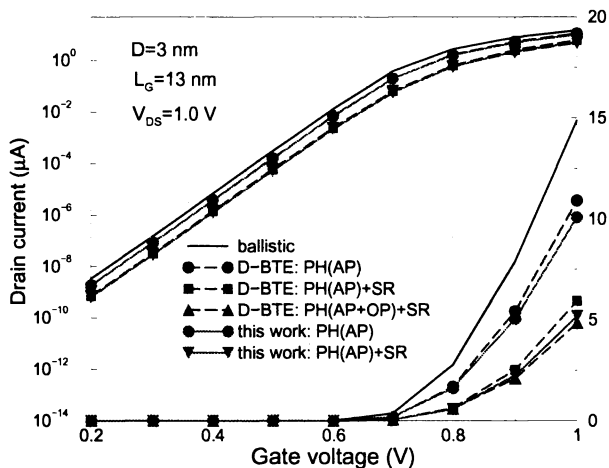


Fig. 4. Log and linear plot of the turn-on characteristics of a 3 nm NW-FET with a gate length $L_g = 13$ nm and an oxide thickness $t_{ox} = 1$ nm according to the present model and a numerical BTE solver from Ref. [9].

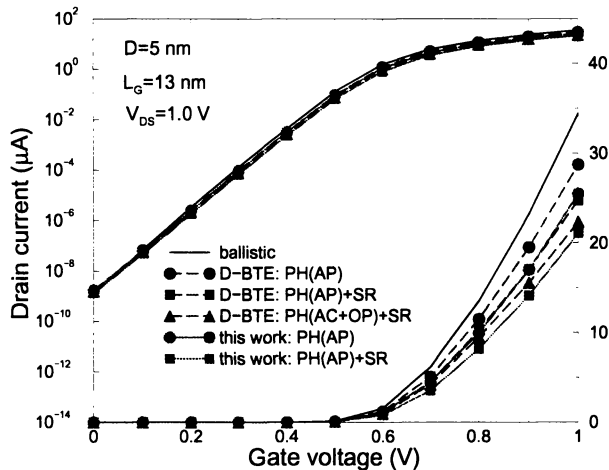


Fig. 5. Log and linear plot of the turn-on characteristics of a 5 nm NW-FET with a gate length $L_g = 13$ nm and an oxide thickness $t_{ox} = 1$ nm according to the present model and a numerical BTE solver from Ref. [9].

due to both inter-subband elastic and inter-valley inelastic collisions. The computations separately account for AP and AP + SR scattering, and the agreement between the two models is nearly perfect in both cases from subthreshold to strong inversion. The slight discrepancy that shows up in strong inversion is thought to be due to the fact that electrons scattered in the upper subbands are unlikely to be backscattered to reach the source, due to the higher energy barrier behind them. In our model, instead, we basically replace an inter-subband scattering with an intra-subband scattering, so that the electron can possibly climb the barrier in its way back to the source. As a result, the simulated current is slightly smaller in our model with respect to that computed with the numerical BTE solver. An additional remark is that, being both computations self consistent, a small deviation in the current flow and electron concentration would modify the electrostatics via Poisson equation, thus yielding a slightly modified electric field along the channel.

The solution of the numerical BTE solver accounting for all scattering mechanisms, including OP, does not greatly deviate with respect to the solution accounting for AP and SR only. If we consider larger-diameter devices, however, the quality of the agreement degrades slightly in strong inversion as shown in figure 5, where the turn-on characteristics of the 5 nm FET are compared. The larger discrepancy is due to the stronger subband interaction enabled by the smaller distance between the subband edges, which makes inter-subband scattering more intense. More specifically, we notice that the present model now predicts a smaller current in strong inversion, with errors as large as 10-12%.

IV. CONCLUSIONS

In this work we have investigated quasi-ballistic transport in NW-FETs by analytically solving the 1D BTE within the assumption of dominant elastic scattering. Inter-subband interactions are accounted for as intra-subband collisions using a suitable weighting factor. The analytic solution is then used to work out closed-form expressions for the nanowire I - V characteristics. As opposed to the 2D case, it is found that the kT -layer plays no role in 1D, and that the backscattering coefficient is a function of the ratio between channel length and momentum-relaxation distance. However, optical phonon emission, neglected in this treatment, is likely to set a limit to the extension of the region beyond the virtual source where backscattering can be effective. This extension is estimated to be $L_{\hbar\omega} + \lambda_{op}$, $L_{\hbar\omega}$ being the distance from the virtual source at which the subband edge drops by the phonon energy $\hbar\omega$, and λ_{op} the phonon-emission mean-free path.

ACKNOWLEDGMENTS

This work has been supported by the EU Integrated Project IST-4-026828 (PULLNANO) via the IU.NET Consortium.

REFERENCES

- [1] M. V. Fischetti, T. P. O'Regan, S. Narayanan, C. Sachs, S. Jin, J. Kim, and Y. Zhang, "Theoretical study of some physical aspects of electronic transport in MOSFETs at the 10-nm gate length," *IEEE Trans. on Electron Devices*, vol. 54, no. 9, pp. 2116–2136, 2007.
- [2] J. P. McKelvey, R. L. Longini, and T. P. Brody, "Alternative approach to the solution of added carrier transport problems in semiconductors," *Phys. Rev.*, vol. 123, no. 1, pp. 51–57, 1961.
- [3] M. Lundstrom, "Elementary scattering theory of the Si MOSFET," *IEEE Electron Device Letters*, vol. 18, no. 7, pp. 361–361, 1997.
- [4] M. Lundstrom and Z. Ren, "Essential physics of carrier transport in nanoscale MOSFETs," *IEEE Trans. on Electron Devices*, vol. 49, no. 1, pp. 133–141, 2002.
- [5] A. Rahman and M. Lundstrom, "A compact scattering model for the nanoscale double-gate MOSFET," *IEEE Tran. on Electron Devices*, vol. 49, no. 3, pp. 481–489, 2002.
- [6] J.-H. Rhee and M. S. Lundstrom, "Drift-diffusion equation for ballistic transport in nanoscale metal-oxide-semiconductor field effect transistors," *J. of Applied Phys.*, vol. 92, no. 9, pp. 5196–5202, 2002.
- [7] A. Rahman, J. Guo, S. Datta, and M. S. Lundstrom, "Theory of ballistic nanotransistors," *IEEE Trans. on Electron Devices*, vol. 50, no. 5, pp. 1853–1864, 2003.
- [8] R. Landauer, "Spatial variation of currents and fields due to localized scatterers in metallic conduction," *IBM J. Res. Dev.*, vol. 32, p. 306, 1988.
- [9] M. Lenzi, A. Gnudi, S. Reggiani, E. Gnani, M. Rudan, and G. Baccarani, "Semiclassical transport in silicon nanowire FETs including surface roughness," *J. of Comput. Electronics, on-line at www.springerlink.com*, 2008.